

File Copy

RESEARCH PROJECT COMPLETION REPORT
OWRR PROJECT NO. A-037-OKLA.

CONCENTRATION GRADIENTS IN AQUIFERS, PHASE II

Submitted to

The Oklahoma Water Resources Research Institute
Oklahoma State University
Stillwater, Oklahoma

Prepared by

Marwin K. Kemp
University of Tulsa

The work upon which this report is based was supported in part by funds provided by the United States Department of the Interior, Office of Water Resources Research, as authorized under the Water Resources Research Act of 1964.

FINAL REPORT

PROJECT: A-037-OKLA

TITLE: "CONCENTRATION GRADIENTS IN AQUIFERS, PHASE II"

PRINCIPAL INVESTIGATOR: Marwin K. Kemp, University of Tulsa

PERIOD: July 1, 1971 - June 30, 1972

ABSTRACT

The objectives of this project were to measure the electrical potential across sodium bentonite membranes due to a thermal gradient using sodium chloride solutions of various concentrations and combine these data with equations derived from the thermodynamics of irreversible processes to predict the rate of electrolyte transport. The electrical potential measurements have shown that for a 1/4" Wyoming Bentonite membrane and sodium chloride solutions, the potential gradient, dE/dT , varies in a log-log fashion with concentration. These data, presented in the table below, can be used to estimate heats of transport, Q^* , for the sodium ion assuming negligible water and chloride ion transport. The heats of transport are also given in the table.

TABLE IX. $Q^*_{Na^+}$ for 1/4" Wyoming Bentonite membranes for several NaCl concentrations

NaCl Conc. (N)	dE/dT (mv/°C)	$Q^*_{Na^+}$ (cal) a.
0.00428	0.153	-1090
0.00856	0.105	-746
0.0171	0.078	-554
0.0342	0.060	-426
0.0513	0.045	-320
0.0684	0.036	-256
0.0856	0.033	-234

The data collected thus far are not sufficient to indicate much about the transport mechanism in the membrane. Thus, the original objective of delineating the role of thermal pumping of electrolytes in the generation of observed concentration gradients in aquifers has not been attained.

FINAL REPORT A-037-OKLA
CONCENTRATION GRADIENTS IN AQUIFERS (PHASE II) - M. K. Kemp

INTRODUCTION:

Water in sedimentary aquifers deep below the surface of the earth is usually salty; sometimes very salty. It is generally assumed that the salt came from ancient oceans in which the sediments were deposited. This assumption is doubtless basically correct, but subsurface waters are usually drastically different in chemical composition from sea water. Some of these waters have 5 to 10,000 mg per liter total dissolved solids, and some of these may have been diluted by surface waters¹. The majority of the waters below a thousand feet or so have a greater concentration of total dissolved solids than sea water with concentrations exceeding 200,000 mg per liter in many cases. Furthermore, the relative amounts of the ions are different from sea water. Sulfate and bicarbonate are usually missing or are present in small amounts. Calcium is usually three times as abundant as magnesium in subsurface waters instead of the opposite trend found in sea water.

The origin of these brines has been the subject of much study and speculation by geochemists². Thus far, it appears that no plausible mechanism has been suggested to account for the observed high salt concentration in the subsurface brines. Some authors have suggested that the high concentration is produced by molecular diffusion of salt from solid salt beds. This explanation seems suspect because the salinity of the subsurface water normally increases with depth whether or not a salt bed is present at greater depths.

The most popular idea at present among the American geochemists is that the compaction of muds to form shales expelled large amounts of water. This water had to pass through other shale beds on its way to the surface, and these beds acted as semi-permeable membranes, retaining the salt. This notion is reasonable and may contain some elements of truth; however, the observed concentration gradients do not seem to fit the estimated volumes of water expelled³.

The influence of gravity on the distribution of solutes has been considered by Russell⁴, Filatov⁵, and Pytkowicz^{6,7}. However, thermodynamic calculations made by Mangelsdorf, Manheim and Gieskes² have shown that gravity alone can not account for the observed concentration gradients. Mangelsdorf, et. al.² pointed out that the calculated effect due to gravity offers a good baseline for considering other effects. Deviations from the effect calculated due to gravitation must be explained by some other means.

The "Soret effect" has been considered by some workers. This effect is the separation of electrolyte in a column of solution due to a thermal gradient. The "Soret effect" leads to an increased concentration of solutes in the colder regions of the solutions for most ions and certainly can not be used to explain the opposite trend in subsurface brines.

Mangelsdorf, et. al.² have published a theoretical treatment of the thermocell diffusion or thermal pumping phenomenon. Tyrell, Taylor, and William⁸ observed that a

synthetic ion-exchange membrane in an electrolyte circuit gives rise to a thermal EMF when a temperature differential is established across it. Shale membranes were shown to exhibit similar behavior by Gondouin and Scala⁹. The hot end of the column was found to be positive with respect to the cold end when cation exchanging particles were used. The positive charge on the hot end of the column will lead to a current flow in the circuit. If the system consists of cation exchanging particles, the current will be equivalent to the movement of cations in or at the surface of the particles toward the hot end of the column. In the external circuit (the solution surrounding the particles) there is a transport of negative ions toward the hot end and a transport of positive ions toward the cold portion of the column. Thus, the amount of electrolyte which migrates to the hot end from the cold end will depend on the relative mobilities of the positive and negative ions in the solution. The portion of the current carried in the external solution by the positive ions results in a circulation of positive charge in the system since positive ions are migrating in the opposite direction on the surface of the particles. However, the portion of the current in the external circuit carried by the negative ions yields a net transport of electrolyte to the hot end since each negative ion that has migrated to the hot end through the solution can join with a positive ion that has migrated along the particle surface to give a "molecule" of electrolyte at the hot end of the column. This results in an increased concentration of electrolyte in that region.

In addition to the interest in the origin of the observed concentration gradients in subsurface brines, there is a considerable interest in the transport of water across membranes due to a thermal gradient (thermoosmosis). Also, the transport of water and salt through soil systems has received some attention. All these transport processes are very likely inter-related and an explanation of one will do much to clarify the mechanisms of the others. Carr and Sollner¹⁰ have experimentally investigated thermoosmosis across some artificial and natural membranes such as cellophane and animal parchment. Considerable experimental and theoretical work by Weeks, et. al.¹¹, Cary^{12, 13}, and Taylor and Cary¹⁴ has failed to fully explain the movement of water and salt through soils. Thermal gradients may play a significant role in such transport processes.

Phase I of this project was begun to experimentally test the theoretical predictions of Mangelsdorf, et. al.². Dilute sodium chloride solutions with Wyoming Bentonite membranes were investigated. Little, if any, electrolyte transport was observed¹⁵ even though EMF measurements indicated an increasing electrical potential with increasing temperature gradient (hot side positive) in agreement with the work of Tyrell, et. al.⁸ and Gondouin and Scala⁹ on other cation exchanging systems. The absence of observed electrolyte transport could be indicative of a slow process. Also, membranes of less than 1/4 inch thickness could not be used in the system; thus, transport might have been impeded due to membrane thickness.

The proposed objectives for this project (Phase II) were a result of the above mentioned observation of negligible transport across the membrane under an imposed thermal gradient. The objectives for Phase II were:

- (1) Measure the electrical potential across a sodium bentonite membrane as a function of membrane thickness, thermal gradient, electrolyte type and electrolyte concentration;

(2) Continue theoretical work on the thermodynamics of irreversible processes in an attempt to correlate thermal gradients, electrical potentials and electrolyte transport; and

(3) Combine the results of (1) and (2) to produce an experimental arrangement and a set of conditions most conducive to electrolyte transport.

THEORETICAL:

The system under consideration consists of two subsystems (') and (") separated by a clay membrane. Across this membrane differences in concentration, pressure, temperature and electrical potential can exist. We assume that each subsystem is well stirred and has uniform values for the variables within each. We will denote the forces due to differences $\Delta\mu$, ΔT , ΔP , $\Delta\psi$ (where μ is the chemical potential, T the temperature, P the pressure and ψ the electrical potential) by the symbol X_i ($i = 1, \dots, n$). These forces give rise to fluxes, J_i ($i = 1, \dots, n$).

The fundamental theorem of the thermodynamics of irreversible processes is that the forces and fluxes may be chosen such that the entropy production of the system conforms to the equation^{16, 17, 18}

$$T \frac{d_i S}{dt} = \sum_{j=1}^n J_j X_j \quad (1)$$

where $\frac{d_i S}{dt}$ is the rate of entropy production due to irreversible processes within the system. The fluxes may be written in terms of the forces, X_k , and a set of phenomenological coefficients, L_{ik} ($i, k = 1, \dots, n$):

$$J_i = \sum_{k=1}^n L_{ik} X_k \quad (2)$$

This set of equations indicates that the flux of the i^{th} species is influenced by the action of each force on each species within the system. The phenomenological coefficients have been shown to satisfy the Onsager reciprocal relations¹⁹

$$L_{ik} = L_{ki} \quad (3)$$

which reduces the number of coefficients which must be determined to predict the fluxes of equation (2).

To evaluate $d_i S/dt$ it is necessary to utilize the laws of conservation of mass and energy and the second law of thermodynamics. The following derivation follows that given by deGroot¹⁶ and by Lakshminarayanaiah¹⁸.

Within the system, subsystem (')/membrane/subsystem("), the conservation of mass requires that

$$dn_k' + dn_k'' = 0 \quad (k = 1, 2, \dots, n) \quad (4)$$

where n_k is the number of moles of species k .

For each subsystem, the conservation of energy is expressed by

$$dU' = d_e U' + d_i U'; \quad dU'' = d_e U'' + d_i U'' \quad (5)$$

and

$$d_i U' + d_i U'' = 0 \quad (6)$$

where $d_i U'$ is the energy exchanged with (") and $d_e U'$ is the energy exchanged by (') and the surroundings. Thus

$$dU = dU' + dU'' = d_e U' + d_e U'' \quad (7)$$

which may be written

$$dU = d_e Q' + d_e Q'' - P' dV' - P'' dV'' \quad (8)$$

if only pressure-volume work is involved. In equation (7) dU gives the total energy absorbed by the whole system, $d_e Q$ is the heat absorbed from the surroundings, and P and V are the pressure and volume terms for the subsystems.

$$d_e U' = d_e Q' - P' dV'$$

$$d_e U'' = d_e Q'' - P'' dV'' \quad (9)$$

since $d_e Q'$ and $d_e Q''$ as well as dV' and dV'' are independent.

A fundamental principle of the thermodynamics of irreversible processes is that the Gibbs equation

$$T dS = dU + P dV - \sum_k \mu_k dn_k \quad (10)$$

is applicable to systems not in thermodynamic equilibrium. Applying this to the two subsystems yields

$$\begin{aligned}
 T' dS' &= dU' + P' dV' - \sum_k \mu_k' dN_k' \\
 T'' dS'' &= dU'' + P'' dV'' - \sum_k \mu_k'' dN_k''
 \end{aligned}
 \tag{11}$$

Substituting equation (5) and the total entropy change in the system

$$dS = dS' + dS'' \tag{12}$$

into equation (11) gives

$$\begin{aligned}
 dS &= \frac{d_e U' + P' dV'}{T'} + \frac{d_e U'' + P'' dV''}{T''} + \\
 &\frac{d_i U'}{T'} + \frac{d_i U''}{T''} - \sum_k \frac{\mu_k' dN_k'}{T'} - \sum_k \frac{\mu_k'' dN_k''}{T''}
 \end{aligned}
 \tag{13}$$

The first two terms are the entropy received from the surroundings. The remaining terms give the production of entropy within the system due to irreversible processes.

$$d_i S = \frac{d_i U'}{T'} + \frac{d_i U''}{T''} - \sum_k \frac{\mu_k' dN_k'}{T'} - \sum_k \frac{\mu_k'' dN_k''}{T''} \tag{14}$$

Incorporating equations (4) and (6) into (14) gives

$$\begin{aligned}
 d_i S &= \frac{d_i U'}{T'} - \frac{d_i U'}{T''} - \sum_k \frac{\mu_k' dN_k'}{T'} + \sum_k \frac{\mu_k'' dN_k'}{T''} \\
 &= -d_i U' \left(\frac{1}{T''} - \frac{1}{T'} \right) + \sum_k dN_k' \left(\frac{\mu_k''}{T''} - \frac{\mu_k'}{T'} \right) \\
 &= -d_i U' \Delta \left(\frac{1}{T} \right) + \sum_k dN_k' \Delta \left(\frac{\mu_k}{T} \right)
 \end{aligned}
 \tag{15}$$

where Δ indicates the difference between (") and (').

The fundamental theorem of the thermodynamics of irreversible processes may be restated as

$$T \left(\frac{d_i S}{dt} \right) = J_u X_u + \sum_{k=1}^n J_k X_k \quad (16)$$

in which J_u gives the energy flux and J_k the mass flux due to all n components in the system. The fluxes may be written as

$$J_u = - (d_i U'/dt) \quad \text{and} \quad J_k = - (dn_k'/dt) \quad (17)$$

Substituting (17) into (16)

$$T(d_i S/dt) = - (d_i U'/dt) X_u + \sum_{k=1}^n [- (dn_k'/dt) X_k] \quad (18)$$

Comparison of (18) with (15) reveals that

$$X_u = T \Delta (1/T) \quad \text{and} \quad X_k = -T \Delta (\mu_k/T) \quad (19)$$

Extending equation (2), the phenomenological law may be written as a linear relation between forces and fluxes giving

$$\begin{aligned} J_i &= \sum_{k=1}^n L_{ik} X_k + L_{iu} X_u \\ J_u &= \sum_{k=1}^n L_{uk} X_k + L_{uu} X_u \end{aligned} \quad (20)$$

in which the Onsager relations

$$L_{ik} = L_{ki} \quad \text{and} \quad L_{ku} = L_{uk} \quad (21)$$

between the phenomenological coefficients are valid.

By defining the energy of transfer U_k^*

$$L_{iu} = \sum_{k=1}^n L_{ik} U_k^* \quad (22)$$

L_{iu} may be eliminated from equation (20). U_k^* is the energy transported by unit flow of k at constant T which means that $X_u = 0$ and $J_k = 1$. Substituting (22) into (20)

$$J_i = \sum_{k=1}^n L_{ik} (X_k + U_k^* X_u) \quad (23)$$

Combining equations (19) and (23) yields

$$J_i = \sum_{k=1}^n L_{ik} \left[\left\{ -T \Delta(\mu_k/T) \right\} + \left\{ U_k^* T \Delta(1/T) \right\} \right] \quad (24)$$

which can be simplified in form by defining

$$\bar{X}_k = \left[-T \Delta(\mu_k/T) + U_k^* T \Delta(1/T) \right] \quad (25)$$

to give

$$J_i = \sum_{k=1}^n L_{ik} \bar{X}_k \quad (26)$$

where the bar ($\bar{\quad}$) indicates the membrane phase.

For cases involving only infinitesimal forces

$$\bar{X}_k = -T d(\mu_k/T) + U_k^* T d(1/T) \quad (27)$$

which can be rearranged to give

$$\bar{X}_k = -d\mu_k - (dT/T)(U_k^* - \mu_k) \quad (28)$$

This may be written

$$\begin{aligned} \bar{X}_k = & -\bar{V}_k dP - RT d \ln a_k - z_k F d\psi \\ & - (dT/T)(U_k^* - H_k^*) \end{aligned} \quad (29)$$

where use has been made of the relations

$$d\mu_k = -\bar{S}_k dT + \bar{V}_k dP + RT d \ln a_k + z_k F d\psi \quad (30)$$

and

$$H_k^* = \mu_k - T\bar{S}_k \quad (31)$$

z_k is the charge (with sign) of the k^{th} species. The difference between U_k^* and H_k^* is called the heat of transport, Q_k^* . Q_k^* is of considerable physical significance as it is the energy transfer per unit transfer of mass and is defined by

$$Q_k^* = U_k^* - H_k^* \quad (32)$$

Combining (32), (29) and (26) yields the general expression for the material fluxes which is given by

$$\begin{aligned} J_i = & \sum_{k=1}^n L_{ik} (-\bar{V}_k dP - RT d \ln a_k \\ & - z_k F d\psi - Q_k^* dT/T) \end{aligned} \quad (33)$$

The interconnections among the various phenomena are shown in Figure 1.²⁰

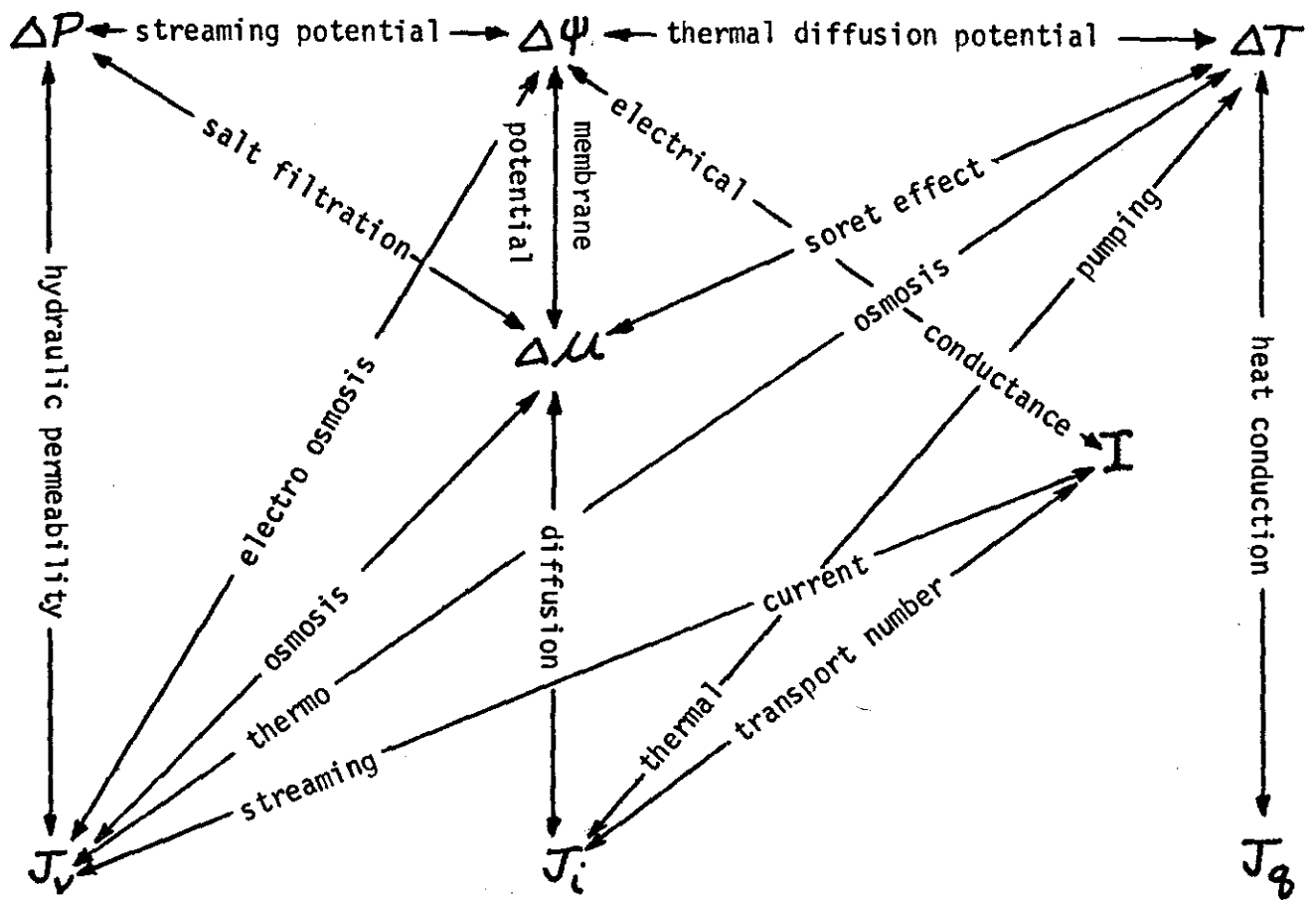


FIGURE 1

The experimental work of this project has been limited to the case in which $dP = 0$, $d \ln a_k = 0$. That is, this work has been concerned with the potential across the membrane as a function of temperature as well as the resulting flux of electrolyte. Under these conditions the flux may be written

$$J_i = \sum_{k=1}^n L_{ik} (-z_k F d\psi - Q_k^* dT/T) \quad (34)$$

The current density for such a system is

$$\begin{aligned}
 I &= F \sum_i z_i J_i \\
 &= \sum_i \sum_k z_i F L_{ik} (-z_k F d\psi - Q_k^* dT/T)
 \end{aligned} \tag{35}$$

or

$$\begin{aligned}
 I &= - \sum_i \sum_k z_i z_k L_{ik} F^2 d\psi \\
 &\quad - \sum_i \sum_k z_i F L_{ik} Q_k^* d \ln T
 \end{aligned} \tag{36}$$

Rearranging

$$d\psi = \frac{-I - \sum_i \sum_k z_i F L_{ik} Q_k^* d \ln T}{+ \sum_i \sum_k z_i z_k L_{ik} F^2} \tag{37}$$

But \bar{K} , the electrical conductance, is given by

$$\bar{K} = - \left(\frac{I}{d\psi} \right)_{dP=0, dT=0, d \ln a_k=0} \tag{38}$$

which, from (36)

$$\bar{K} = \sum_i \sum_k z_i z_k L_{ik} F^2 \tag{39}$$

Hence

$$d\psi = \frac{-I - \sum_i \sum_k z_i F L_{ik} Q_k^* d \ln T}{\bar{K}} \tag{40}$$

The transference number is given by

$$\begin{aligned}
 \bar{t}_k &= (F z_k J_k / I)_{dP=0, dT=0, d \ln a_k=0} \\
 &= \frac{F \sum_i z_i z_k F L_{ik} d\psi}{\sum_i \sum_k z_i z_k L_{ik} F^2 d\psi} \\
 &= \frac{F^2 \sum_i z_i z_k L_{ik}}{\sum_i \sum_k z_i z_k L_{ik} F^2}
 \end{aligned} \tag{41}$$

which, on comparison with (39) gives

$$\bar{t}_k = \frac{F^2 \sum_i z_i z_k L_{ik}}{\bar{K}} \tag{42}$$

Rewriting (40)

$$\begin{aligned}
 d\psi &= -(I/\bar{K}) - \frac{1}{F} \sum_i \sum_k \left[\frac{z_k z_i F^2 L_{ik} Q_k^* d \ln T}{z_k \bar{K}} \right] \\
 &= -(I/\bar{K}) - \frac{1}{F} \sum_k \frac{\bar{t}_k}{z_k} Q_k^* d \ln T
 \end{aligned} \tag{43}$$

In the system under study the current is zero, whence

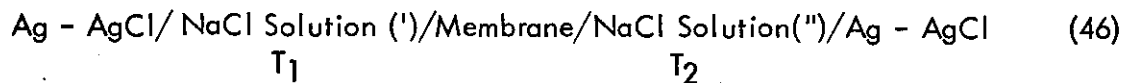
$$d\psi = -\frac{1}{F} \sum_k \frac{\bar{t}_k}{z_k} Q_k^* d \ln T \tag{44}$$

For a negatively charged membrane the negative co-ions are effectively excluded from the membrane. Hence, for a single electrolyte it can be assumed that all the current is carried by the positive counter ions, which in the case of sodium chloride solution is the sodium ion. Thus

$$d\psi \approx -\frac{1}{F} \frac{t_{Na^+}}{(t+1)} Q_{Na^+}^* d \ln T \approx -\frac{1}{F} Q_{Na^+}^* d \ln T$$

$$\frac{d\psi}{d \ln T} \approx -\frac{Q_{Na^+}^*}{F} \quad \text{or} \quad \frac{d\psi}{dT} \approx -\frac{Q_{Na^+}^*}{FT} \quad (45)$$

For a cell such as



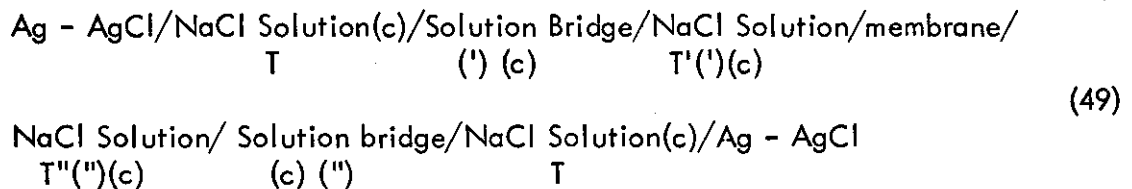
involving reversible electrodes the cell potential may be written

$$dE = dE_{rev} + d\psi \quad (47)$$

For cell (46), $d\psi$ can not be experimentally determined due to the temperature effect on dE_{rev} . dE/dT has been expressed by Lakshminarayanaiah²¹ as

$$\frac{dE_{rev}}{dT} = \frac{\Delta S^\circ}{F} - \left(\frac{R}{F}\right) \ln a_{Cl^-}'' - \left(\frac{RT}{F}\right) \frac{d \ln a_{Cl^-}''}{dT} \quad (48)$$

However, if the electrodes can be maintained at the same temperature as in cell (49)



$\frac{dE_{rev}}{dT}$ will be zero. The only factors now interfering with the direct evaluation of $Q_{Na^+}^*$ are

- (i) junction potential across solution bridge (')
- (ii) contact potentials, and
- (iii) thermoelectric effects in the leads.

Both (ii) and (iii) may be negligible and, hopefully, (i) can be estimated. Hence the cell

potential may be written from (47)

$$\frac{dE}{dT} = \frac{d\psi}{dT} + \frac{dE_J}{dT} \quad (50)$$

or

$$\frac{dE}{dT} = - \frac{Q_{Na^+}^*}{FT} + \frac{dE_J}{dT} \quad (51)$$

where E_J is the junction potential for solution bridge ("). Upon evaluation theoretically of dE_J/dT , $Q_{Na^+}^*$ may be estimated directly from plots of E vs T which may be determined in cell (49). It should be noted that the above has assumed all transport is due to the sodium ions. This may not be the case as suggested by Lakshminarayanaiah¹⁸. Water transport itself may be involved in which case equation (51) must be modified to give (assuming $t_{Cl^-} = 0$)

$$\frac{d\psi}{dT} = - \frac{1}{FT} \bar{t}_{Na^+}^* Q_{Na^+}^* - \frac{1}{FT} \bar{t}_{H_2O}^* Q_{H_2O}^* + \frac{dE_J}{dT} \quad (52)$$

where

$$\bar{t}_k^* = (\bar{t}_k / z_k) = F^2 \sum_i z_i L_{ik} / R \quad (53)$$

Equation (52) is subject to the restraint that

$$\sum_k z_k \bar{t}_k^* = 1 \quad (54)$$

The relative importance of $\bar{t}_{H_2O}^*$ and $\bar{t}_{Na^+}^*$ remains to be determined.

EXPERIMENTAL:

A. Electrode Plating

In order to measure the electrical potential, it was essential to prepare stable and reproducible silver-silver chloride electrodes. The electroplating procedure described by Ives and Janz²² was used to produce electrodes which were not stable or reproducible. The electrodes seemed to be smooth on visual examination and they seemed to be working properly. However, it was found that neither stability nor reproducibility was maintained. Unplated dots were noticed on the electrode when they were observed through a magnifying glass. Many plating attempts were made using different current densities for different trials of electroplating but satisfactory results were not obtained. It was concluded that the cleaning procedure was not adequate. After trying a variety of solvents and solutions to improve the cleaning procedure the following satisfactory procedure was found:

The platinum electrodes were cleaned with boiling concentrated nitric acid and washed with water. They were polished with fine alumina using a brush, then cleaned with alkali solution (KOH) using a brush and washed thoroughly with running water. Alkali cleaning is an essential part of the cleaning procedure, without which desired electrodes cannot be obtained. This cleaning ensures that the surface of the electrode is not water repelling.

Following the cleaning, the electrodes were subjected to a silver strike. Silver strike is important in that using very high current density for a few seconds gives a quick and even silver deposition on the electrode which in turn helps even plating. A simple apparatus can be sketched as shown in Figure 2.

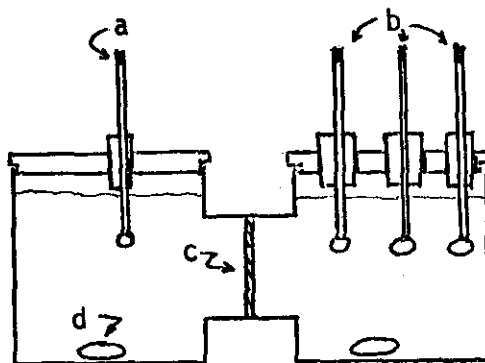


FIGURE 2. Cell plating apparatus.
a - platinum anode; b - electrodes
to be plated; c - porous plate; d -
magnetic stirring bar

The silver strike solution was made up by adding to one liter of water

2.2 to 2.4 g $\text{KAg}(\text{CN})_2$
65 to 67 g KCN
25 to 27 g K_2CO_3

A current density of 20 to 25 amps/ft^2 was passed for 20 to 30 seconds.

After silver strike it is not desirable to rinse the electrodes since electrode plating is a quite delicate operation and the number of operations should be reduced as far as possible. The apparatus and procedure was the same as for the silver strike. The solution for plating was prepared by adding 33 to 34 g each of K_2CO_3 , KCN and $\text{KAg}(\text{CN})_2$ to one liter of water. A current density of 2 to 3 amps/ft^2 was passed through the cell for about 2 hours.

The final operation required was chloridization to produce a AgCl layer on the electrode. A part of silver deposited on the electrode was converted to silver chloride by using 0.1 N HCl solution and current density of 1 to 2 amps/ft^2 for 30 minutes.

The electrodes produced by this method were reproducible and stable in the range of 0.0 to 0.06 mv.

B. EMF Measurements

The apparatus used is shown in the Figure 3. The cell is divided into two compartments by means of porous metal plates between which a clay membrane is packed. Both compartments were filled with a given concentration of NaCl solution. The membrane material was prepared by gradual slurring of montmorillonite (Wyoming Bentonite) with a NaCl solution of the same concentration as in the cell. The mixture was stirred until a thick slurry was obtained. This slurry was packed between the two porous stainless steel plates to form the cell membrane.

Glass tubing served as the solution bridges between the cells and the electrode compartments. One end of the salt bridge was inserted in the solution of a compartment and the other in the solution of the same concentration in the separate beaker in which a previously plated Ag-AgCl electrode was inserted. The two electrodes in two beakers were connected to the potentiometer. The two beakers carrying the two electrodes were kept in a waterbath to keep the electrodes at the same temperature.

The temperature of the compartments were controlled separately by using thermostats, control relays and heating coils. A cooling coil was employed in the low temperature side to offset heat transport through the membrane from the hot side. Temperatures were measured using precise thermometers and at any temperature control was maintained to $\pm 0.1^\circ\text{C}$. Stirring was accomplished by use of magnetic stirring bars.

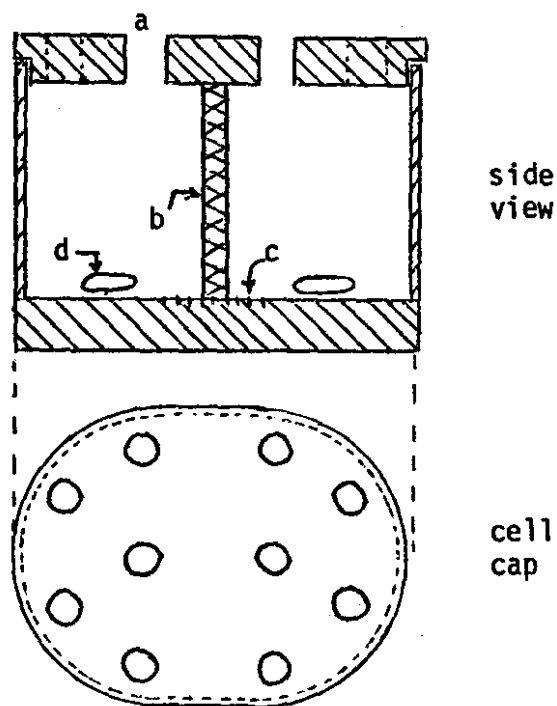


FIGURE 3a. EMF measurement cell. a - openings for thermoregulator, salt bridge, thermometer, heater, cooling coil; b - porous stainless steel supports and membrane; c - grooves for membrane supports; d - magnetic stirring bars.

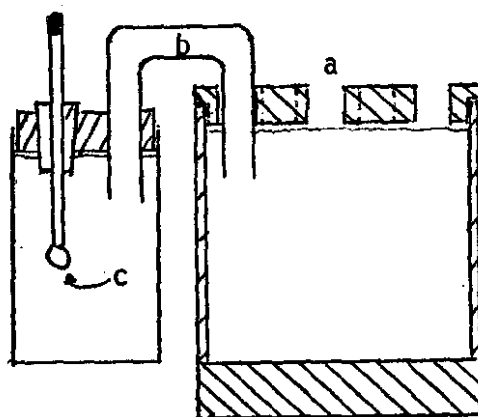


FIGURE 3b. Cell, salt bridge and electrode compartment. a - probe openings; b - salt bridge; c - Ag/AgCl electrode

After setting up the apparatus as described above, the whole system was allowed to come to equilibrium. It generally took about 3 to 4 hours for equilibrium to be established. In the beginning of the experiment, the temperature of both the compartments was kept the same so the potential difference should theoretically be zero. This was not always the case due to slight differences in the electrodes and, perhaps, to non-equilibrium in the membrane. However, since the object of this work was to find E vs. ΔT , a non-zero E at $\Delta T = 0$ is not significant as long as no changes occur during the time required for measurement.

Initial potential at equal temperature was noted and the temperature of one compartment was raised gradually in increments of about one degree centigrade. The temperature of the compartment in which there was a cooling coil was kept essentially constant throughout the experiment. After every raise of temperature, the system was allowed to establish equilibrium which took about 5 to 7 minutes. At every ΔT , the potential was measured and recorded. This was continued up to the point when the temperature difference of the two compartments reached about 20°C . The graph of temperature difference (ΔT) against potential (E) was plotted. These experiments were repeated for different concentrations. In all cases the potential measured is good to approximately ± 0.05 mv.

RESULTS AND DISCUSSION

The experimental values for E vs. ΔT are summarized in Tables I - VII for a 1/4" Wyoming Bentonite membrane and various concentrations of NaCl solutions. These data are plotted in Figures 4 and 5. The slopes of the lines in Figures 4 and 5 are tabulated in Table VIII. Figure 6 is a plot of $\Delta E / \Delta T$ vs. solution concentration. As can be seen in Figure 7, there is apparently a log-log relationship between the function $\Delta E / \Delta T$ and the concentration. This, of course, does not imply that such would be the case for other electrolytes.

The data presented in Table VIII may be used to calculate the heat of transport of Na^+ through the membrane if several assumptions are made. Assuming the transference of Cl^- is negligible as is to be expected in a negatively charged membrane we may apply equation (52). Two other approximations are necessary to estimate $Q_{\text{Na}^+}^*$. The first is that dE_j/dT is small. This is probably a good assumption since over small temperature ranges the transference number differences between Na^+ and Cl^- do not change dramatically. Finally, we must assume that $\bar{t}_{\text{H}_2\text{O}}^* \approx 0$. The validity of this assertion remains to be determined. Under these rather stringent conditions equation (52) reduces to

$$\frac{dE}{dT} = - \frac{Q_{\text{Na}^+}^*}{FT} \quad (55)$$

Equation (55) has been utilized to calculate the values of $Q_{\text{Na}^+}^*$ given in Table IX. For comparison similar calculations have been made for data of other workers using similar

TABLE I. E vs. ΔT for 1/4" Wyoming Bentonite membrane and 1/4 g/l NaCl solution. (See Figure 4)

$T_1(^{\circ}\text{C})$	$T_2(^{\circ}\text{C})$	$\Delta T(^{\circ}\text{C})$	E (mv)
36.1	27.7	8.4	0.0
37.5	28.0	9.5	0.20
38.6	27.7	10.9	0.40
40.2	27.7	12.5	0.60
41.4	27.7	13.7	0.80
42.75	27.7	15.05	1.00
44.0	27.8	16.2	1.19
45.4	27.55	17.75	1.48
46.7	27.7	19.0	1.68
48.0	27.9	20.1	1.86
49.4	27.8	21.6	2.02

TABLE II. E vs. ΔT for 1/4" Wyoming Bentonite membrane and 1/2 g/l NaCl solution. (See Figure 4)

$T_1(^{\circ}\text{C})$	$T_2(^{\circ}\text{C})$	$\Delta T(^{\circ}\text{C})$	E (mv)
29.4	29.4	0.4	0.24
31.2	29.4	1.8	0.34
32.5	29.4	3.1	0.50
33.8	29.4	4.4	0.62
35.2	29.5	5.7	0.76
36.5	29.5	7.0	0.90
37.9	29.5	8.4	1.04
39.2	29.5	9.7	1.17
40.5	29.6	10.9	1.30
41.8	29.6	12.2	1.44
43.5	29.7	13.8	1.60
44.6	29.7	14.9	1.73
45.8	29.7	16.1	1.86

TABLE III. E vs. ΔT for 1/4" Wyoming Bentonite membrane and 1 g/l NaCl solution. (See Figure 4)

$T_1(^{\circ}\text{C})$	$T_2(^{\circ}\text{C})$	$\Delta T(^{\circ}\text{C})$	E (mv)
35.8	32.5	3.3	0.01
37.0	32.6	4.4	0.10
38.5	33.1	5.4	0.18
39.9	33.1	6.8	0.29
41.0	33.3	7.7	0.36
42.5	33.5	9.0	0.46
43.8	33.7	10.1	0.54
45.2	34.3	10.9	0.61
46.4	34.4	12.0	0.70
47.7	34.6	13.1	0.78
49.0	34.8	14.2	0.84
50.5	34.8	15.7	0.84

TABLE IV. E vs. ΔT for 1/4" Wyoming Bentonite membrane and 2 g/l NaCl solution. (See Figure 4)

$T_1(^{\circ}\text{C})$	$T_2(^{\circ}\text{C})$	$\Delta T(^{\circ}\text{C})$	E (mv)
30.8	28.7	2.1	0.75
32.0	28.7	3.3	0.84
33.5	28.6	4.9	0.93
34.8	28.6	6.2	1.00
36.2	28.7	7.5	1.06
37.4	28.6	8.8	1.14
38.8	28.8	10.0	1.22
40.1	28.7	11.4	1.31
41.5	28.8	12.7	1.39
42.7	28.7	14.0	1.48
44.0	28.7	15.3	1.56
45.4	28.8	16.6	1.64

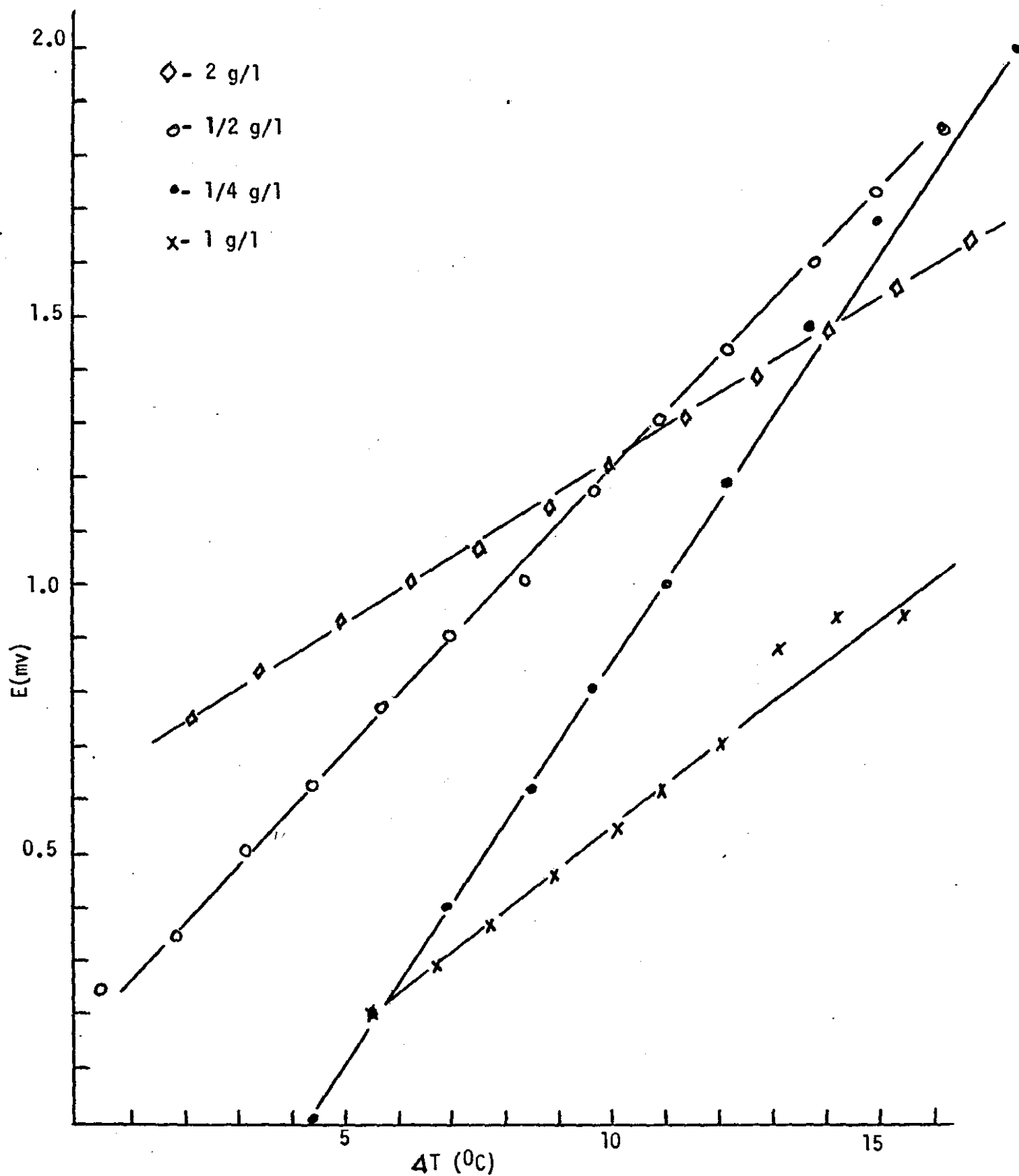


FIGURE 4. E vs. ΔT for various concentrations of NaCl solutions. $1/4$ " Wyoming Bentonite membrane.

TABLE V. E vs. ΔT for 1/4" Wyoming Bentonite membrane and 3 g/l NaCl solution. (See Figure 5)

$T_1(^{\circ}\text{C})$	$T_2(^{\circ}\text{C})$	$\Delta T(^{\circ}\text{C})$	E (mv)
31.25	28.65	2.60	-0.29
32.5	28.65	3.85	-0.24
33.85	28.65	5.20	-0.18
35.25	28.65	6.60	-0.12
36.5	28.65	7.85	-0.06
37.9	28.65	9.25	-0.00
39.2	28.65	10.55	+0.13
40.65	28.65	12.00	+0.20
41.95	28.65	13.30	+0.25
43.35	28.65	14.70	+0.29
44.6	28.65	15.95	+0.35
45.85	28.85	17.00	+0.40

TABLE VI. E vs. ΔT for 1/4" Wyoming Bentonite membrane and 4 g/l NaCl solution. (See Figure 5)

$T_1(^{\circ}\text{C})$	$T_2(^{\circ}\text{C})$	$\Delta T(^{\circ}\text{C})$	E (mv)
33.9	34.4	- 0.5	0.2
35.2	34.4	0.8	0.30
36.6	34.4	2.2	0.36
38.0	34.4	3.6	0.42
39.3	34.4	4.9	0.48
40.7	33.3	7.4	0.57
42.0	31.9	10.1	0.68
43.3	31.6	11.7	0.74
44.6	31.5	13.1	0.79
45.9	31.5	14.4	0.83
47.2	31.5	15.7	0.88
48.5	31.5	17.0	0.92
49.9	31.4	18.5	0.97
51.1	31.4	19.7	1.01
52.4	31.4	21.0	1.07

FIGURE 5. E vs. ΔT for various concentrations of NaCl solutions. 1/4" Wyoming Bentonite membrane.

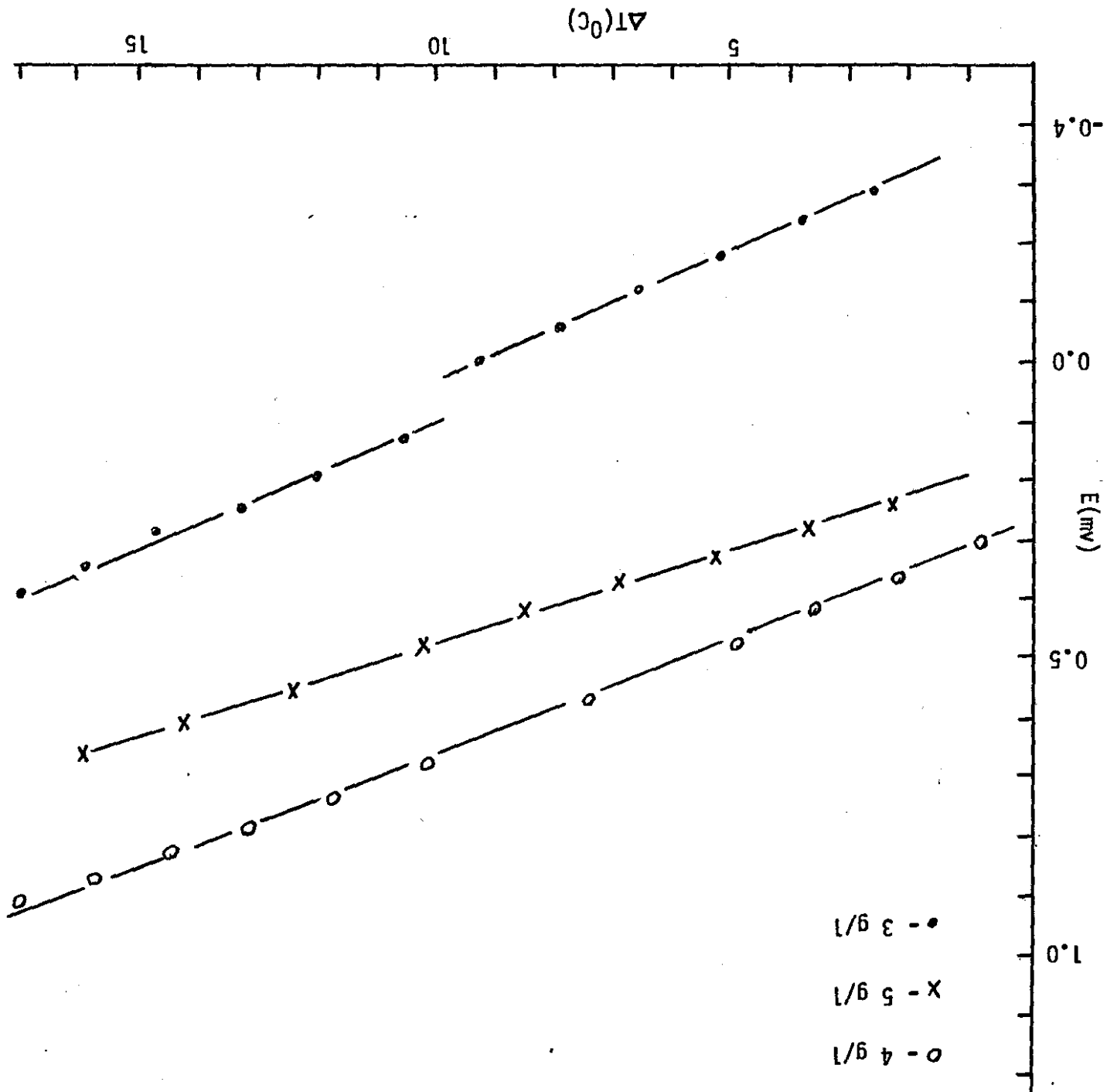


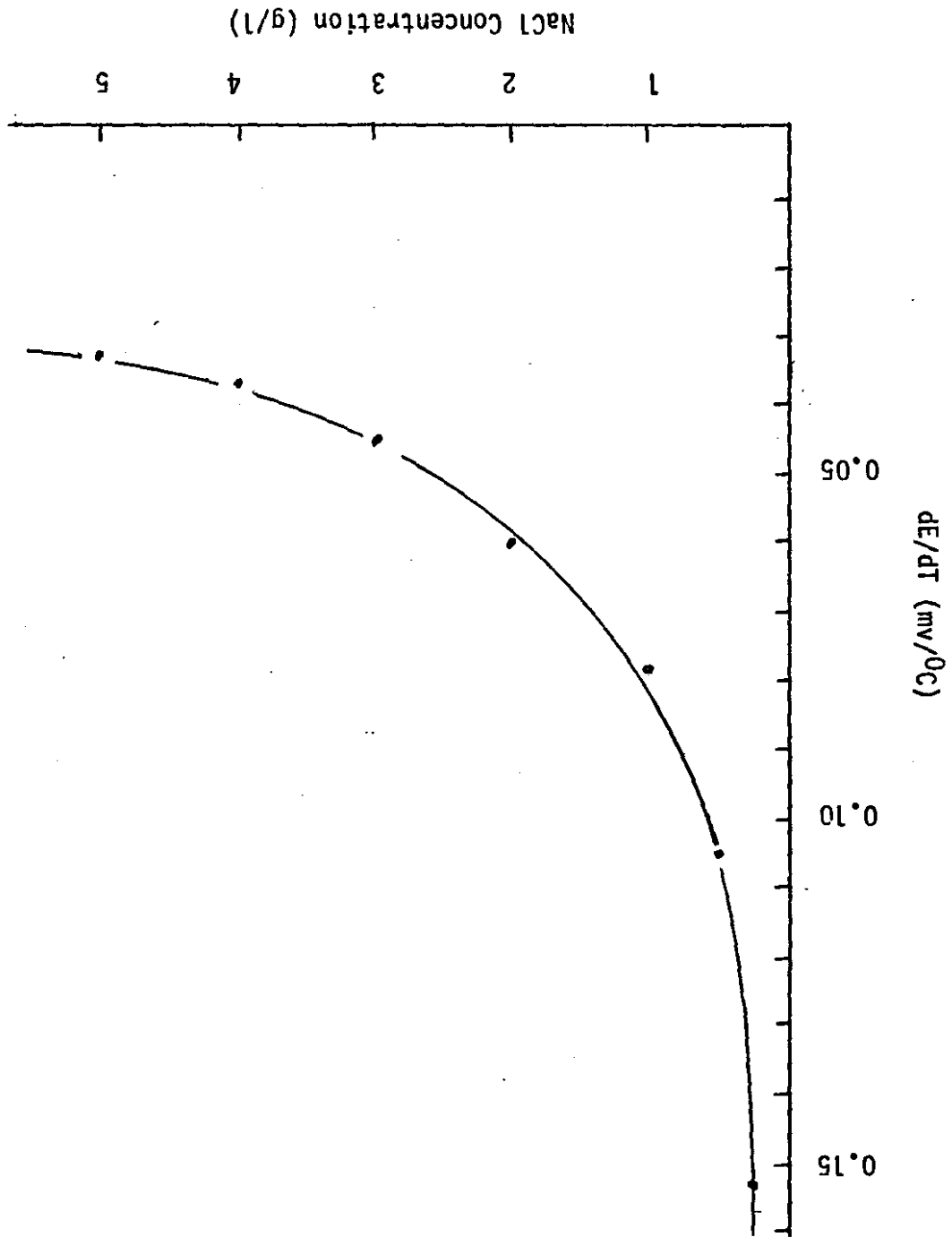
TABLE VII vs. ΔT for 1/4" Wyoming Bentonite membrane and 5 g/l NaCl solution. (See Figure 5)

$T_1(^{\circ}\text{C})$	$T_2(^{\circ}\text{C})$	$\Delta T(^{\circ}\text{C})$	E (mv)
29.5	27.2	2.3	0.24
31.2	27.5	3.7	0.28
33.4	28.1	5.3	0.33
35.2	28.3	6.9	0.37
37.5	29.0	8.5	0.42
39.2	29.0	10.2	0.48
43.2	30.8	12.4	0.56
45.0	30.8	14.2	0.62
46.7	30.8	15.9	0.67
48.5	30.8	17.7	0.73
50.4	30.8	19.6	0.79

TABLE VIII. Slopes, $\Delta E/\Delta T$ for various NaCl concentrations and 1/4" Wyoming Bentonite membranes. (See Figures 6 and 7)

Concentration g/l	Slope (mv/ $^{\circ}\text{C}$)
1/4	0.153
1/2	0.105
1	0.078
2	0.06
3	0.044
4	0.036
5	0.033

FIGURE 6. dE/dT vs. NaCl concentration for 1/4" Wyoming Bentonite membrane.



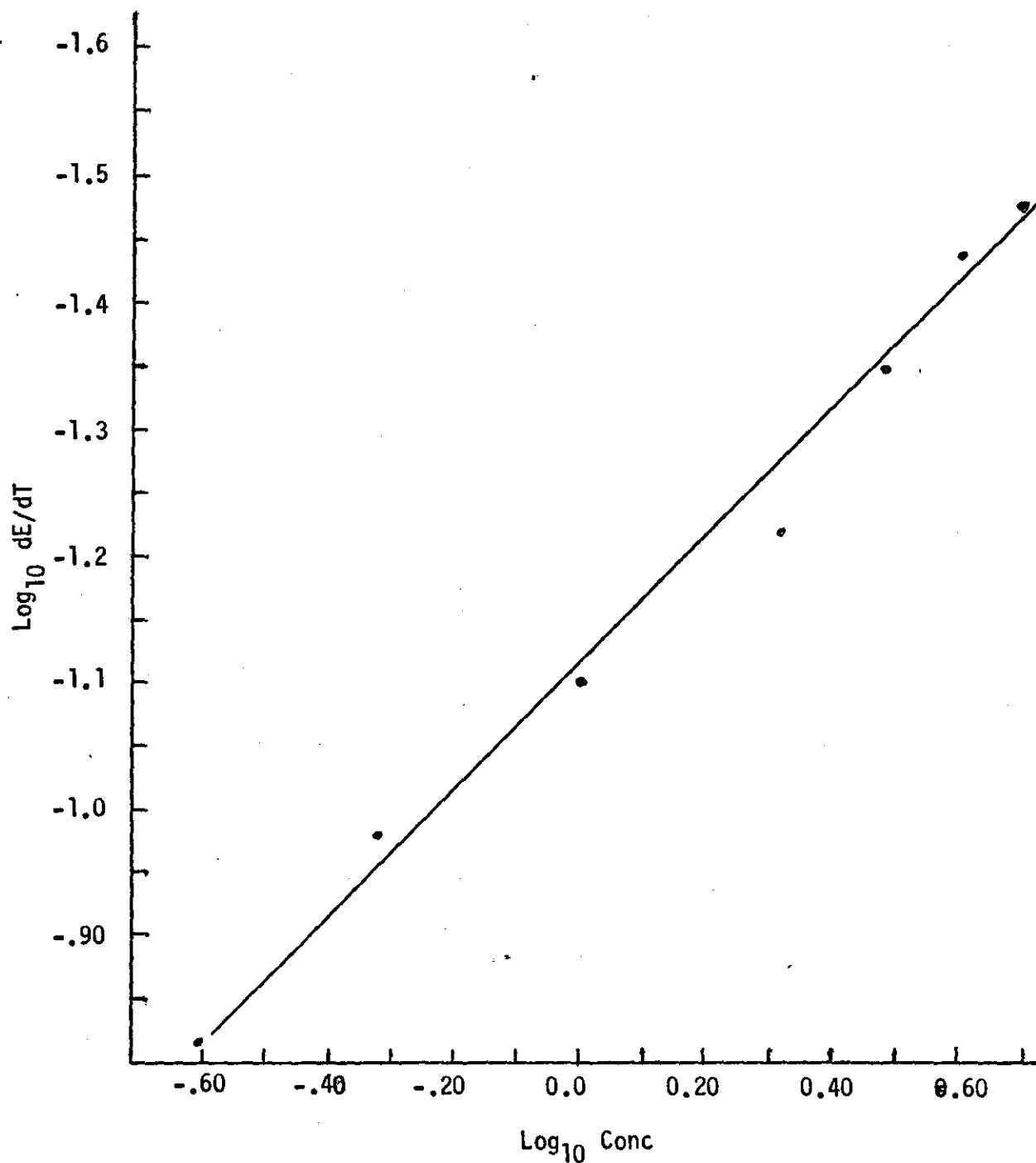


FIGURE 7. Log dE/dT vs. Log Concentration for NaCl solutions and 1/4" Wyoming Bentonite membrane. (dE/dT in $\text{mv}/^{\circ}\text{C}$, conc. in g/l)

TABLE I. $Q^*_{Na^+}$ for 1/4" Wyoming Bentonite membranes for several NaCl concentrations

NaCl Conc. (N)	dE/dT (mv/°C)	$Q^*_{Na^+}$ (cal) a.
0.00428	0.153	-1090
0.00856	0.105	- 746
0.0171	0.078	- 554
0.0342	0.060	- 426
0.0513	0.045	- 320
0.0684	0.036	- 256
0.0856	0.033	- 234

a. T chosen as approximately $T_{avg} = 308$ °C

TABLE X. Q^* for several different cations

M^+	Q^* (cal)				References and Notes
	1.0 N	0.1 N	0.01 N	0.001 N	
K^+ (KCl)	+1400	+2800	+4200	+5500	8. Cation exchange resin 'Permaplex C10' used as membrane.
Na^+ (Na Br)	+1100	+2300	+3700	+5000	
Li^+ (Li Cl)	+ 710	+2100	+3500	+4800	
Na^+ (NaCl)	- 710	-2100	-2600		9. Shale membrane
K^+ (KCl)		- 175			23. Collodion membrane. Agar-Agar salt bridges used.
Na^+ (NaCl)		- 220	- 720		This work

TABLE XI. Q^* for several cations in 0.01 N solution

M^+	Q^* (cal) from Reference						This Work
	18	8	9	24	25	26	
K^+	670	+4200	--	300	2600	-1550	--
Na^+	370	+3700	-2600	270	2300	-1800	-720
Li^+	0	+3500	--	30	0	-3020	--

experimental approaches. These results are tabulated in Table X for several concentrations. Table XXXIV of Lakshminarayanaiah¹⁸ giving the relative heats of transfer calculated by several workers is reproduced in Table XI for 0.01 N solutions. Also included in Table XI are selected values from Table X and an interpolated value from Table IX.

All that can be said for these data is that the values of different workers follow the same trend. There is by no means agreement even on the sign of Q^* . Much work remains to be done to eliminate the uncertainties that arise due to different sets of assumptions. It is encouraging that the trends are the same and the fact that the values themselves do not agree is not unexpected since different membrane types are involved. The effect of membrane type needs further investigation.

Work is continuing in this laboratory to find Q^* for other electrolytes. Also, the effect of membrane thickness is being investigated. Membrane thickness will, of course, affect the rate of electrolyte transport but should have negligible effect on the EMF produced. After definite trends are established for the values of Q^* then perhaps the transport mechanism can be discussed. If this can be accomplished for one particular system then a giant step will have been taken toward explaining electrolyte transport across any charged membrane.

CONCLUSION:

The first two objectives for this project, namely:

- 1) Measure the electrical potential across a sodium bentonite membrane as a function of membrane thickness, thermal gradient, electrolyte type and electrolyte concentration;
- 2) Continue theoretical work on the thermodynamics of irreversible processes in an attempt to correlate thermal gradients, electrical potentials and electrolyte transport

have been partially accomplished. Continued work is required since only NaCl has been studied thus far. Also, various membrane thicknesses are to be utilized. However, this work has shown that consistent potential data can be obtained and can be used with some approximations to estimate heats of transport. The validity of these approximations need further study.

It is anticipated that continued work will lead to a better understanding of the transport mechanisms for electrolytes across charged membranes. If so, then the ultimate objective of both Phase I and Phase II of this project which was to explain the role of thermal pumping of electrolytes in establishing observed concentration gradients in aquifers may be attainable. It is not possible at the present time.

REFERENCES:

1. Parke A. Dickey, *Amer. Assoc. Petroleum Geologist Bulletin*, 50, 2472 (1966).
2. P.C. Mangelsdorf, Jr., F.T. Manheim and J.M.T.M. Gieskes, *ibid*, 54, 617 (1970).
3. Parke A. Dickey, *Chemical Geology (Elsevier)*, 4, 361 (1969).
4. W.L. Russell, *Amer. Assoc. Petroleum Geologists Bulletin*, 17, 1213 (1933).
5. K.V. Filatov, *Gidokhimiicheskie Materialy*, 24, 85 (1955).
6. R.M. Pythowicz, *Limnology and Oceanography*, 7, 434 (1962).
7. *Ibid*, 8, 286 (1963).
8. H.J.V. Tyrell, D.A. Taylor and C.M. Williams, *Nature*, 177, 668 (1956).
9. M. Gondouin and C. Scala, *Am. Inst. Mining and Metallurg. Engineers Trans. (Petroleum)*, 213, 1701 (1958).
10. Charles W. Carr and Karl Sollner, *J. Electrochem. Soc.*, 109, 616 (1962).
11. L.V. Weeks, S.J. Richards and J. Letcy, *Soil Sci. Soc. Am. Proc.*, 32, 193 (1968).
12. J.W. Cary, *ibid*, 30, 428 (1966).
13. J.W. Cary, *Soil Sci.*, 100, 168 (1965).
14. S.A. Taylor and J.W. Cary, *Soil Sci. Soc. Am. Proc.*, 28, 167 (1964).
15. M.K. Kemp, Oklahoma State University, Water Resources Research Institute, Research Project Technical Report, 1971 (OWRRA-025-OKLA).
16. S.R. deGroot and P. Mazur, "Thermodynamics of Irreversible Processes", North Holland Publishing Co., Amsterdam, 1951.
17. I. Prigogine, "Introduction to Thermodynamics of Irreversible Processes", Interscience Publishers, 1961.
18. N. Lakshminarayanaiah, *Chem. Rev.* 65, 491 (1965).
19. Lars Onsager, *Phys. Rev.*, 37, 405 (1931); 38, 2265 (1931).
20. G.J. Hills, P.W. M. Jacobs and N. Lakshminarayanaiah, *Nature*, 179, 96 (1957).

21. N. Lakshminarayanaiah, Ph.D. Thesis, University of London, 1956.
22. J.G. David Ives and George J. Janz, "Reference Electrodes", Academic Press, New York, 1961, pp. 204-207.
23. Toshio Ikeda, J. Chem. Phys. 28, 166 (1958); 31, 267 (1959).
24. E.D. Eastman, J. Am. Chem. Society, 48, 1482 (1926); 50, 283, 292 (1928).
25. K. Wirtz, Z. Physik, 124, 482 (1948).
26. J.C. Goodrich, F.M. Goyan, E.E. Morse, R.G. Preston, and M.B. Young, J. Am. Chem. Soc., 72, 4411 (1950).